

Simulation-Driven Design Optimization: A Case Study on a Double 90° Elbow Bend

Richard A. Adjei and Ali Mohsin

Abstract—Flow through elbow bends are found in many engineering applications. The complexity of pipe systems and the high demand for efficiency and accuracy poses a challenge for traditional engineering design. Commercially, industries spend much more time in the design phase of components, using different simulation methods, in order to get the best possible design and save time in service. However, the question of how to readily explore a large number of design alternates for optimal solutions remains even a greater challenge in traditional product design methodology. This paper demonstrates how faster design processes, by means of unique parametric modeling, direct coupling, automation, and application of optimization techniques, can be used to explore complex shapes and designs. As a case study, a fully parametric model of a double 90° bend was designed, and directly coupled with CFD tool for analysis of flow fields. Parameterization methods for describing the complex pipe bend geometry were discussed which provide required flexibility and smoothness by a minimum set of descriptive parameters. Shape optimization was subsequently performed to determine parameters that affect the performance of the pipe. It was observed that the optimum case showed a relatively larger distribution of total pressure at mid-stream outer walls with very low pressures far upstream and downstream region compared to the localized pressure distribution of baseline design. Flow velocity was seen to be higher at downstream of optimum case due to the change in bend shape and high momentum flow of the fluid. The optimum case showed a percentage decrease of 19.83% in total pressure, and an increase of 1.03% in outlet flow uniformity compared to baseline design.

Index Terms—Double 90° bend, direct coupling, optimization, parametric modeling.

I. INTRODUCTION

Fluid flow, such as air, water, and oil through pipe bends has been of considerable interest for industrial piping systems. Flow in bends is affected by complex parameters, such as centrifugal forces, turbulence formation, secondary flows, friction and pressure on outer walls on bends. One important parameter for this flow is the Dean number, which can be defined by the Reynolds number Re and the curvature ratio d of the pipe bend. When the Dean number is high, the flow may become unsteady, and separation may take place. For a comprehensive depiction of the flow, it would be highly desirable to solve the Navier Stokes equations. Furthermore, there are situations where the experiments for these bends configurations are very difficult to be carried out and with significant cost, especially for large bends. Focus has been

turned to the techniques of computational fluid dynamics (CFD) in order to simulate the flow [1], [2].

Simulation-driven design is seen as the major technology leap in product development and engineering. The success story of computer aided design (CAD) already started many years ago. During the last decade, computational fluid dynamics (CFD) has become a major asset for product development too [3]. The necessary step forward now is the tight integration of both CAD and CFD. This allows the investigation of hundreds and even thousands of variants in automated processes, the clear benefits being faster processes and better products.

Recent studies show the extensive use of CFD and optimization tools for the analysis of elbow bends. Reference [4], presented pressure loss data for a series of pipe bends with various curvature radius using CFD calculations from four turbulence models. Reference [5] and [6] performed CFD predictions of dilute gas- solid flow through a curved 90° duct bend based on a Differential Reynolds Stress Model (DRSM) for calculating turbulent flow quantities and a Lagrangian particle tracking model for predicting solid velocities. Reference [7], in his paper on elbow pipe design optimization of an oil and gas pipeline system, conducted reliability design studies and optimization using the Monte Carlo simulation. Design optimization was conducted to obtain the minimum wall thickness of elbow pipe such that the system reaches certain reliability levels which have been determined with minimum installation cost without violating constraints. Hence, the key parameters optimized were the thickness of the pipe and installation cost, holding all other parameters constant. Also, [8] simulation and optimization of sixteen possible combinations of three parameters, temperature, and friction coefficient and flow velocity in a hot pushing pipe bending process were analyzed by the orthogonal testing method. Aimed at the uniform wall-thickness of elbow pipes, the best parameter of hot pushing pipe bending process were at a temperature of 750°C, flow velocity of 4 m/s, and friction coefficient of 0.16. To the author's best of knowledge, the use of simulation-driven design for analysis and optimization of a large number of geometry variants in an automated process to obtain an optimum or set of optimum elbow bend designs meeting the desired efficiency has rarely been researched.

In this paper, a double 90° elbow bend is used as a case study to demonstrate how simulation-driven design can be used to optimize complex geometries. A parametric double 90° elbow was designed using unique parametric definitions and functional surfaces. CFD analysis was performed to determine flow field parameters such as total pressure drop, flow velocity and uniformity index of the pipe bend. Direct CAD-CFD coupling approach was used to link the geometry and CFD result files for design automation and optimization.

Manuscript received May 30, 2014; revised August 23, 2014. This work was supported in part by the FRIENDSHIP SYSTEMS GmbH, Benzstrasse 214482 Potsdam, Germany. The authors are with Nanjing University of Aeronautics and Astronautics, Nanjing, China (e-mail: adj.richard@hotmail.com, mohsin07mt@gmail.com).

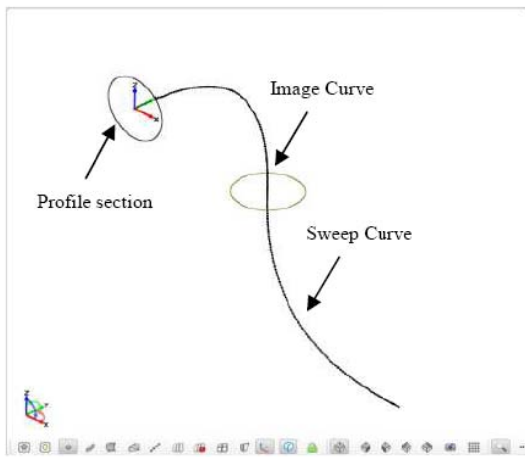


Fig. 1. Profile section of the double 90° bend.

II. GEOMETRY DESIGN APPROACH

A. Elbow Parametric Modeling

The double 90° elbow geometry was designed using a CAE tool, the FRIENDSHIP Framework. The parametric model was designed using a parametric section curve. Fig.1 shows the profile section of the double 90° bend. The section profile was described by the width (axis A) and height (axis B) of an ellipse, having a radius of 1m, with respect to a global coordinate system. A planar b-spline curve, which runs from the center of profile curve, is used to create a 3D-path (also known as a trajectory), along which the contour curve will be swept. An image of the profile curve is subsequently created that utilizes a sweep transformation in order to sweep along the path. Translation of the image curve is realized by making it dependent on a transformation entity where values for Δx , Δy and Δz move the curve within the Cartesian space. A path parameter is set on the image curve which is used in a feature definition for surface generation. This will be discussed in the following section.

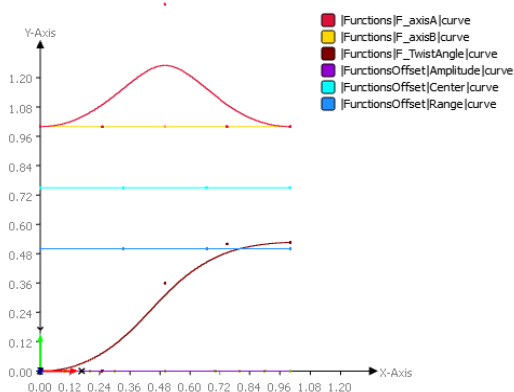


Fig. 2. Function distributions for profile parameters.

B. Parameter Distribution

The profile parameters can now be considered as not being constant but rather as being dependent on further entities in a longitudinal direction of the elbow bend. Individual distributions are created which describe the parameter values within a certain range. In this example, the xy -system is chosen as reference system and the curves are supposed to be

functions of x , i.e.

$$y_i = f_i(x), \quad (1)$$

i denoting the parameter index. Surface creation was realized by extruding the 2D-profile along the z -axis (for which Δz comes into play). Therefore, each parameter distribution f_i can be interpreted as a function of z ,

$$p_i = p_i(z) \quad (2)$$

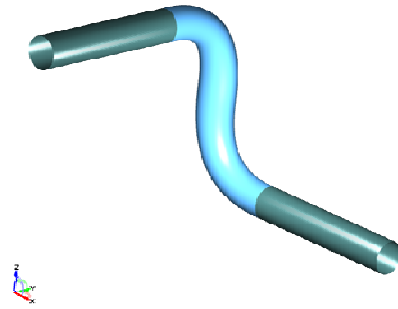


Fig. 3. Meta-surface of pipe elbow and extensions.

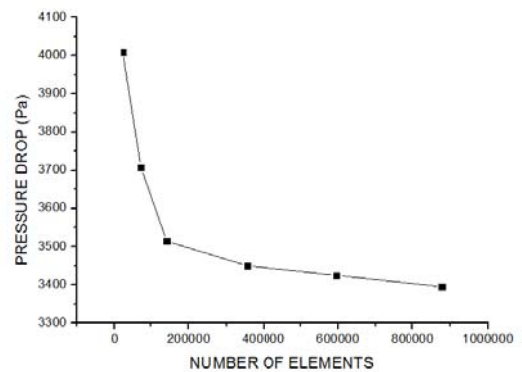


Fig. 4. Grid independence study.

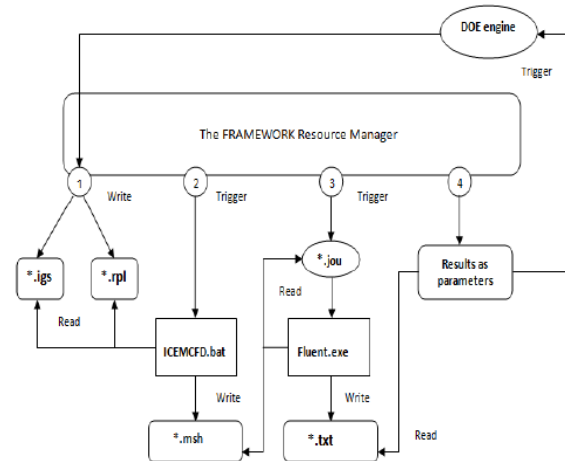


Fig. 5. CAD-CFD direct coupling flow process.

Fig. 2 depicts distributions in the xy -system for each profile parameter: The function curve with the sinusoidal profile defines the tube twist at the elbow from upstream through to the downstream of the pipe. Control of the width and height of the ellipse profile was defined by axis A and B curves respectively. These curves vary the shape of the entire double elbow while the horizontal curves; section amplitude,

range and center provide a constant profile area along the pipe. Initially, translation in x - and y -direction is given by a constant zero-function. For z -translation of the profile, a linear distribution is designed that will provide the required z -values for extrusion purposes. Note again that these functions are just suppliers of ordinate values with regard to discrete abscissa values. So far, there is no reference to the profile parameters or the feature definition [10], [11].

C. Surface Generation

The profile description given as feature definition and its parameter distributions need to be related to each other for surface generation. This is done by means of the key entity curve engine. The feature definition simple profile, the ellipse curve, is chosen and the base curve is assigned, i.e. the single curve which actually describes the profile. The object editor of the curve engine supplies each accessible parameter of the definition so that any meaningful distribution can be set, either a distribution curve or just a scalar value. Additionally, a factor is applied for each parameter curve ([function, factor]) for convenience e.g. When normalized distributions are used.

The curve engine and their functions are based on the global xy -coordinate system which is required in order to know about abscissa and ordinate axis. All functions are defined in the interval $[0, 1]$. By means of this input data, the curve engine is now ready to compute ordinate values at arbitrary abscissa values $x \in [0, 1]$, transfers them to the feature definition and provides the corresponding profile on request. Surface creation itself is done via the meta-surface object. For this novel surface type, the configured curve engine has to be set, together with two abscissa values for the generation range. Such an abscissa value is called base position and refers, again, to the coordinate system of the chosen curve engine and its functions. This set of information finally provides the closed mathematical definition of the surface [11].

D. Design Variables

For the geometry variations, 9 design variables were specified (related to the points describing the curves), as follows:

TABLE I: DESIGN PARAMETERS OF DOUBLE 90° ELBOW PIPE

Variables	Upstream	Midstream	Downstream
Group 1	US_Weight	Mid_Axis A	DS_Weight
Group 2	US_Axis A	Mid_Axis B	DS_Axis A
Group 3	US_Axis B	US_Dent	DS_Axis B

Where US and DS weight represent control points that change the shape of the elbow curve at upstream and downstream. Axis A and Axis B represent the width and height of the ellipse profile at upstream, mid-stream and downstream. Each design variable corresponds to a point in y -axis of the xy - coordinate system.

III. CFD SETUP AND SIMULATION

A. Mesh and Boundary Conditions

In order to increase accuracy and save computation time, grid independence study was performed. This was to help

determine the grid element threshold beyond which the change in computational results was minimum. Fig. 4 shows a chart of the grid independence study. It was observed that elbow mesh with elements within the ranges of 20,000 to 75,000, 75,000 to 145000 and 350,000 to 600,000 had a percentage decrease of 7.5, 5.2, and 0.7 percent in total pressure drop respectively. Hence, grid generated for the baseline simulation had a total of 427517 tetrahedral mesh elements with 3 prism layers.

B. Flow Model

The flow in elbow bend was treated as a steady flow of a viscous, incompressible (i.e., constant density), and isothermal liquid, with the working fluid being water.

Gravitational effects were ignored, for which the density and viscosity of water are $\rho = 998.2 \text{ kg/m}^3$, and $\mu = 1.003 \times 10^{-3} \text{ kg/m.s}$. The flow velocity at the inlet, as averaged over the pipe cross section, is assumed to be $U_{avg} = 5 \text{ m/s}$. This results in a Reynolds number of

$$Re = \frac{\rho U_{avg} D}{\mu} \cong 9.95 \times 10^6 \quad (3)$$

Which indicates that the flow can be expected to be fully turbulent. Though turbulent flows are inherently unsteady, it is the prediction of the mean, or averaged, properties of the flow that is typically of most interest.

From the studies of [1], three dimensional steady state Reynolds Averaged Navier Stokes (RANS) equations were solved using the segregated implicit solver. The right choice of a turbulence model is a critical when an industrial turbulent flow problem is faced, especially when this problem involves three dimensional flow phenomena, which need an accurate modeling. In this paper, the RANS equations were computed using the Reynolds stress model (RSM) instead of the k - ζ model. Although the k - ζ model is robust, efficient and very widely used; it is known that in highly swirling flows or in flows where significant stream curvature exists, this model becomes inadequate. In such cases, the RSM generally offers greater accuracy by modeling the Reynolds stresses directly.

Non-equilibrium wall functions were used for the treatment of the near wall layer. Because of the capability to partly account for the effects of pressure gradients and departure from equilibrium, the non-equilibrium wall functions are recommended for use in the complex flows involving separation, reattachment, and impingement where the mean flow and turbulence are subjected to severe pressure gradients and change rapidly. The second order scheme was used for the RANS equations calculations, with a pressure-velocity coupling achieved using SIMPLEC algorithm. The default under relaxation factors were used to aid convergence for all models.

C. Evaluations and Objectives

To evaluate the computations and to drive the DOE algorithm, several performance metrics were monitored. The total pressure drop (ΔP_t) was used as the single objective.

Total pressure drop (ΔP_t), velocity (w) and uniformity index (γ) at the outlet were determined using the following equations:

$$\Delta P_t = P_{tin} - P_{tout} \tag{4}$$

$$\gamma = 1 - \frac{\sum_{i=1}^n \frac{\sqrt{(w_i - \bar{w})^2}}{\bar{w}} * A_i}{2 * n * A} \tag{5}$$

where P_{tin} , P_{tout} , γ , w_i , \bar{w} , A_i , A and n are total pressure at inlet and outlet, uniformity index, local velocity, mean velocity, local cell area, total cell area and number of cells respectively.

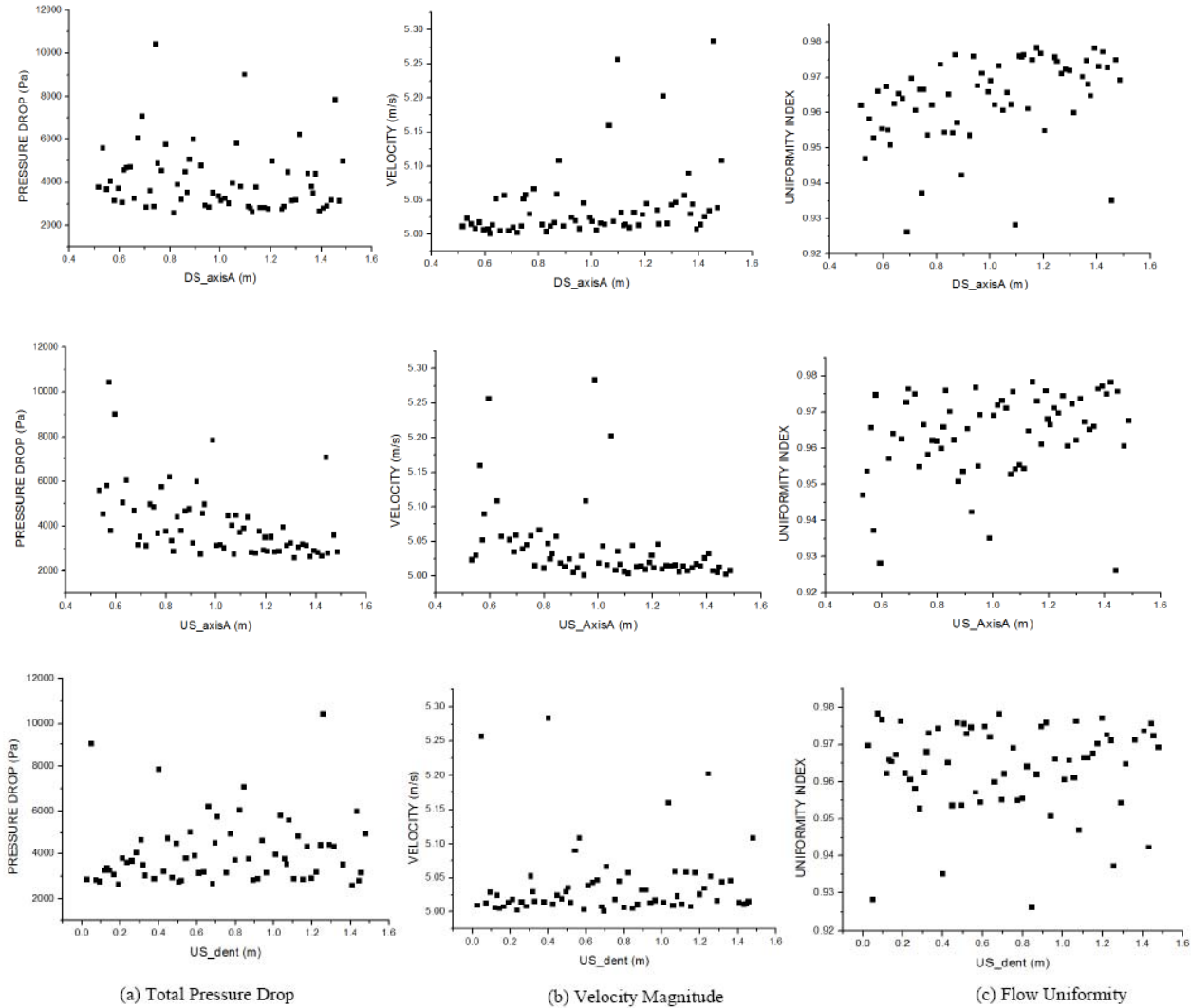


Fig. 6. Charts showing the influence of some key variables on total pressure drop, velocity magnitude and flow uniformity.

IV. DIRECT CAD-CFD COUPLING APPROACH

A set of mechanisms allow the integration of external software that is required for the individual design process. The direct CAD-CFD coupling consists of a CAE tool, FRIENDSHIP Framework (FFW), ICEMCFD and ANSYS Fluent solver. Fig. 5 shows the direct CAD-CFD coupling process. Generic integration methodology was employed for parsing, reading and replacement of functionality for arbitrary ASCII input and output files with editors available in graphical user interface. Geometry export of the elbow bend was used to generate a mesh for CFD analysis. A script, which captures the mesh process and file directories, was auto-generated during meshing.

In performing the CFD analysis, files such as journal, text, case and data files that capture simulation setup and results were used to directly link input and output files to the executables of ICEMCFD and Fluent so that when triggered in batch mode via a batch file, the scripts and files are run in an automated manner. Absolute export and import file paths

in scripts and files were changed to relative paths in order for generated geometries to be correctly selected for each automated run.

V. VARIATION AND OPTIMIZATION STRATEGY

A. Design of Experiment

To perform optimization, the parametric geometry and the CFD simulation results were linked to FFW built-in variation and optimization engines. A DoE was run for 70 variants using a Sobol sequence (quasi-random investigation of the design space) considering 9 design variables and 3 evaluation parameters. This engine generates pseudo-random numbers based on a deterministic calculation. The resulting numbers are spread in a uniform manner across the domain space of the variable. Here, the entire domain space of a design situation gets checked initially.

B. Design Optimization

The results were then evaluated and the best variant was

identified. The Tangent Search (T-Search) single-objective optimization was conducted for 120 variants, starting with the best case identified in the DoE. The T-Search is a reliable optimization engine for small scaled optimization problems.

It detects a decent search direction, ensures fast improvements in that direction and keeps the search within the feasible solution space.

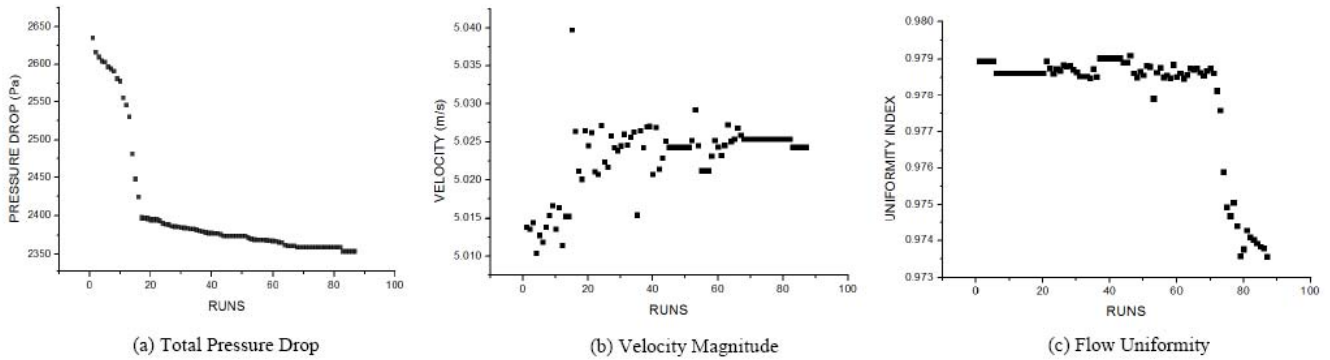


Fig. 7. Charts showing the optimization of total pressure drop, velocity magnitude and flow uniformity against number of runs.

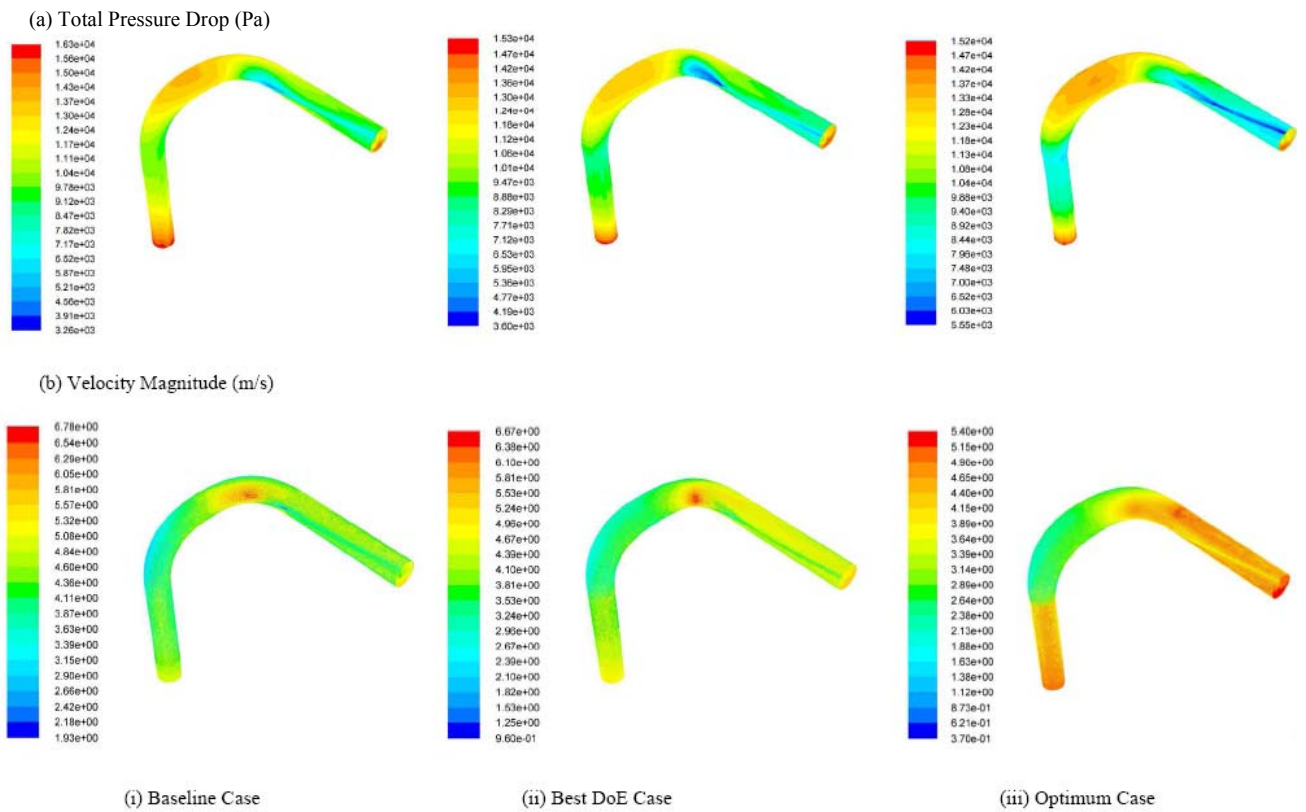


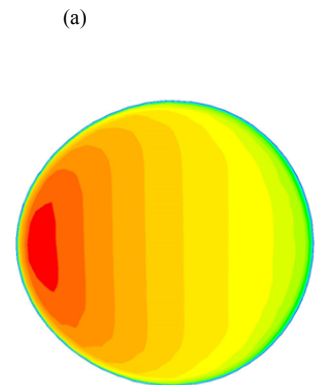
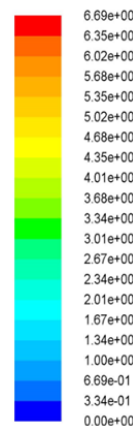
Fig. 8. Pressure and velocity contours of baseline, best DoE and optimum design case.

VI. RESULTS AND DISCUSSION

A. DoE Using Sobol Sequence

The main evaluation parameters exhibited a strong positive correlation. The best variants in terms of total pressure drop were also best in terms of flow velocity and flow uniformity at the outlet. Considering the influence of some design variables on the ΔP_t , it was observed from fig.6a that the downstream elbow height and upstream elbow dent variable had only a mild influence on ΔP_t . The upstream elbow height showed a partly uniform distribution of pressure drop of design cases over a range of 0.5m to 1.5m having a few designs with relatively higher pressure drop compared to baseline. Likewise, the upstream dent variable experienced a similar trend of ΔP_t but over a range of 0.1m to 1.5m.

Velocity Contours (m/s)



(I) Elbow bend upstream.

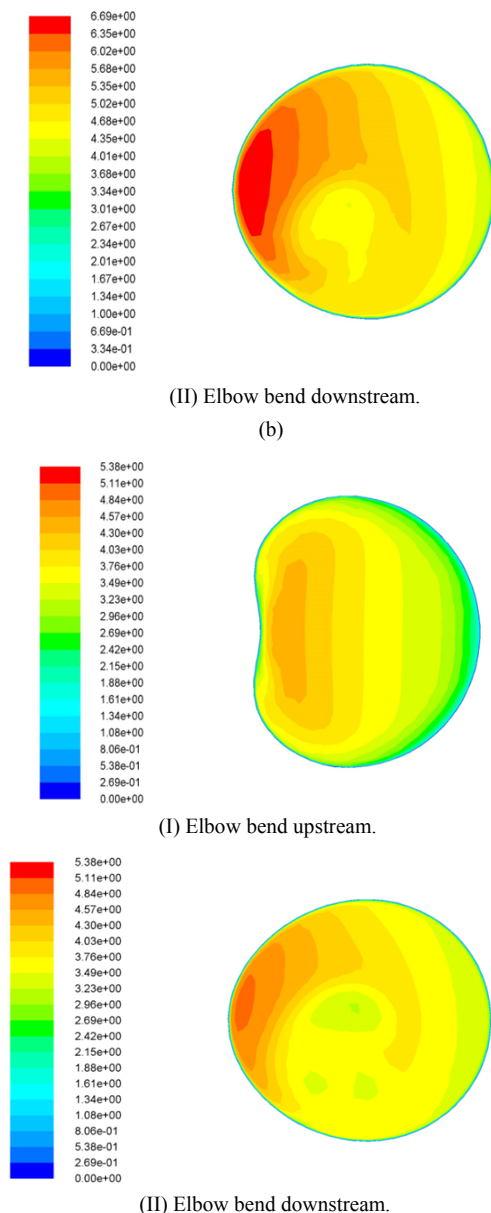


Fig. 9. Velocity contours of (a) baseline and (b) optimum design case elbow bend cross-section at upstream and downstream.

The width variable of both upstream and downstream influenced performance and the best designs were far from the baseline. However, the upstream width variable had the largest influence on ΔP_t . The ΔP_t decreased with increasing upstream elbow width, corresponding to an outlet velocity percentage increase of 0.3 and flow uniformity increase of 0.4 with a larger number of design cases having higher flow uniformity compared to downstream width variable. The best 4 variants in terms of total pressure drop were selected as starting point for T-Search single objective optimization.

B. Design Optimization

Fig. 7 shows optimization charts of total pressure drop, velocity magnitude and flow uniformity against number of design variants (runs). It was observed that there was an abrupt decrease in total drop from baseline design to initial DoE design for T-search optimization during run. However, total pressure drop from the DoE initial start to T-Search best case showed a near linear to constant decrease with convergence around 89 for the 120 design variants. Similar trends were observed for both flow uniformity and Velocity

magnitude during the T-search optimization. However, initial T-search variants for velocity magnitude had no correlation but rather clustered close to the initial DoE case distributed towards the optimum variants. Flow uniformity, on the other hand, showed a fair correlation distribution of variants towards the best case.

Flow losses in a piping system result from a number of system characteristics, which include; internal pipe friction, changes in direction of flow, obstructions in flow path, and sudden or gradual changes in the cross-section and shape of flow path. Fig.8 shows pressure and velocity distribution of baseline, DoE and optimum design cases. The baseline design shows a localized pressure distribution at mid stream with relatively lower pressures far upstream and downstream region. This is because, when the flow enters upstream through to elbow section, the faster moving portion of the fluid near the center axis move outward from the centerline due to inertial effects, resulting in a general migration from the inner toward the outer walls of the bend. Across the elbow joint, the fluid can be said to have entered the viscous boundary layer on the outer wall, and returns toward the inner wall in a form of a swirl or loop. This vortical flow behavior are secondary flows that circulate in opposite directions within the top and down halves of the pipe. The resulting streamline pattern shows a separation zone after the bend downstream which is consistent with the results in [9]. The velocity contour, as seen in Fig. 8(i), indicates a larger low velocity region located at the downstream from the separation point. Flow velocity is seen to be higher at the inner walls of the elbow joints due to the bend and high momentum flow of the fluid. The flow attached to the inner and outer walls recovers to uniform with a nearly constant gradient at approximately 2.5d downstream of the bend.

This phenomenon is also observed in the DoE best case and optimum case. However, the optimum case shows a larger distribution of pressure at mid-stream outer walls with very low pressures far upstream and downstream region. The velocity contour, on the other hand, indicates high velocity regions located at the upstream and downstream. This is possibly due to the change in shape of the flow path; 1.69% increase in weight of bend downstream and 15.13% decrease in weight of bend upstream (Table. I). From the principle of mass conservation, a change in cross-sectional area, from a larger region to a smaller region, will result in higher average velocity downstream. This is evident in Fig.8(b). The transition point of pressure gradient moves towards the outlet of downstream bend on the outer wall but keeps almost unchanged along the curvature on the inner wall. Further downstream, counter-rotating vortices, caused by the centripetal force, are formed and creates a lower pressure streamline pattern from elbow joint to outlet along the inner walls. The adverse pressure gradient at the outer wall, which results in excess friction at the bend and also from the flow separating from the inner wall, significantly affects pressure drop across the pipe. The optimum case showed a percentage decrease of 19.83% in ΔP_t , and an increase of 1.03% in outlet flow uniformity compared to baseline design.

Also, to illustrate the nature of flow distribution at the elbows of the pipe, Fig. 9 shows a two-dimensional in-plane velocity contours in the cross-section normal to the centerline at the midpoint of the elbow. Each vector is color-coded according to the magnitude of the full three-dimensional

velocity. The generally higher velocity on the inner wall is evident for both cases. However, a much lower flow velocity, with a fairly uniform distribution at upstream elbow bend, is observed in the optimized design. This is possibly due to the relative increase in cross-sectional area (height and width) and the presence of a dent at the inner walls. The thickness of the relatively slow moving boundary layer on the outer wall increases significantly. This means an increased in spacing

between the contours, or possibly a reduced wall shear stress. Flow contours downstream show a non-uniform distribution from center to inner wall with baseline case having higher velocity than the optimum case. The faster moving fluid, from Fig. 9(a), is displaced toward the inner wall of the pipe. This is typically the result of the main flow having separated from the surface.

TABLE II. CFD AND OPTIMIZATION RESULTS OF BASELINE CASE, DOE BEST CASE AND OPTIMUM DESIGN CASE

Design(m)	Mid_Axis A	Mid_Axis B	DS_Weight	US_Weight	US_Dent	DS_Axis A	DS_Axis B	US_Axis A	US_Axis B	Total Pressure Drop (Pa)	Velocity (m/s)	Uniformity Index
Baseline	1.000	1.000	0.707	0.707	0	1.000	1.000	1.000	1.000	2936.134	5.016	0.968
DOE 12	1.313	1.281	0.994	0.644	1.406	0.813	1.188	1.313	1.063	2609.381	5.014	0.974
OPT 74	1.5	1.283	0.719	0.600	1.500	1.087	1.364	1.489	1.268	2353.755	5.024	0.978

VII. CONCLUSION

An optimization study for a double 90° elbow bend was conducted using an initial Sobol sequence exploration of the design space, followed by a T-Search strategy. The following conclusions were drawn:

- The optimized geometry was substantially improved compared to the baseline: 19.83% in ΔP_t , and 1.03% in outlet flow uniformity.
- The design variables with the most influence were those describing the height and width at both upstream and downstream.
- Further performance improvements seem likely if the design variable bounds are increased. Additional design variables can be introduced to fine-tune the elbow bend (e.g. speed of transition of the section shape).
- The direct coupling of friendship-framework with ICEMCFD and Fluent is very effective for fluid dynamic optimization of internal flows.

ACKNOWLEDGMENT

R. A. Adjei would like to thank Mike Saroch of the friendship systems GmbH for his support in geometry modeling and guidance in the completion of this research paper.

REFERENCES

[1] L. Wang, D. Gao, and Y. Zhang, "Numerical simulation of turbulent flow of hydraulic oil through 90° circular sectional bend," *Chinese Journal of Mechanical Engineering*, p. 3901, 2012.

[2] T. A. Mikhail, Walid A. Aissa, S. A. Hassanein, and O. Hamdy, "CFD simulation of dilute gas-solid flow in 90° square bend," *Energy and Power Engineering*, vol. 3, pp. 246-252, July 2011.

[3] *The Friendship-Framework: Software for Simulation, Driven Design*, Friendship Systems GmbH, 2013, pp. 1

[4] N. Crawford, S. Spence, and A. Simpson, "A numerical investigation of the flow structures and losses for turbulent flow in 90° elbow bends," in *Proc. IMechE, Part E: J. Process Mechanical Engineering*, 2009, vol. 223, no. 1, pp. 27-44.

[5] W. Yang and B. T. Kuan, "Experimental investigation of dilute turbulent particulate flow inside a curved 90° bend," *Chemical Engineering Science*, vol. 61, no. 11, 2006, pp. 3593-3601.

[6] B. T. Kuan, "CFD simulation of dilute gas-solid two-phase flows with different solid size distributions in a curved 90° duct bend," *The Australian and New Zealand Industrial and Applied Mathematics*, vol. 46, 2005, pp. C744-C763.

[7] S. M. Yusuf, "Elbow pipe design optimization of oil and gas pipe system owned by joint operation body Pertamina-petrochina east java (job p-PEJ) tuban based on reliability," B.S. Thesis, Dept. Ocean Eng, Institut Teknologi SEPULUH Nopember, Surabaya, 2010.

[8] X. Y. Lu, Q. T. Zhou, L. L. Huang, and J. M. Liu, "Numerical simulation and parameter optimization of hot pushing elbow pipe," *Applied Mechanics and Materials*, vol. 432, no. 92, pp. 92-97.

[9] G. F. Homicz, "Computational fluid dynamic simulations of pipe elbow flow," Sand Report, Sandia National Laboratories Albuquerque, New Mexico 87185 and Livermore, California 94550, SAND2004-3467, pp. 7-9.

[10] M. Brenner, C. Abt, and S. Harries, *Feature Modeling and Simulation-Driven Design for Faster Processes and Greener Products*, ICCAS 2009, Shanghai, China.

[11] J. Palluch, A. Starke, and S. Harries, "Parametric modeling for optimal components in turbomachinery," in *Proc. Worldwide Turbocharger Conference*, vol. 40, 2009.

[12] C. Abt and S. Harries, "Direct coupling of CAD and CFD for the design of functional surfaces," *NAFEMS Seminar: 'Simulation Driven Design - Potential and Challenges'*, Wiesbaden, Germany, March 2008.

[13] R. R. Hilleary, "The tangent search method of constrained minimization," Technical Report, Naval Postgraduate School, Monterey, California. March 1966, no. 59



Richard A. Adjei received his B.Sc degree in 2011 in materials engineering from the University of Ghana, Ghana. He is presently pursuing a masters degree in materials engineering at the Nanjing university of Aeronautics and Astronautics, China, with research interest in thermal analysis, simulation and design optimization of aerostructures and materials.



Ali Mohsin received his B.E degree in 2011 in metallurgy and materials engineering from Mehran University of Engineering and Technology, Pakistan. He is presently pursuing a masters degree in materials engineering at the Nanjing university of Aeronautics and Astronautics, China, with research interest in polymeric composites for aerospace and bioengineering applications.